Plant Cell Reports (2019) 38:545–558
https://doi.org/10.1007/s00299-019-02385-2

ORIGINAL ARTICLE

Abnormal tapetum development and energy metabolism associated with sterility in SaNa-1A CMS of *Brassica napus* L.

Kun Du[1] · Yuyue Xiao[1] · Qier Liu[1] · Xinyue Wu[1] · Jinjin Jiang[1] · Jian Wu[1] · Yujie Fang[1] · Yang Xiang[2] · Youping Wang[1]

Received: 24 November 2018 / Accepted: 23 January 2019 / Published online: 31 January 2019

Abstract

Key message **Abnormal tapetum degradation and anther development in cytoplasmic male sterility SaNa-1A are the main reasons for the anther abortion.**

Abstract SaNa-1A is a novel cytoplasmic male sterility (CMS) line of *Brassica napus* derived from somatic hybrids of *B. napus*-*Sinapis alba*, and SaNa-1B is the corresponding maintainer line. Ultrastructural comparison between developing anthers of sterile and maintainer lines revealed abnormal subcellular structure of pollen mother cells (PMCs) in the CMS line. The PMC volume and size of nucleus and nucleolus in the CMS line were smaller than those in the maintainer line. The abnormal tapetum cell development and delayed tapetum degradation inhibited microspore development. Finally, anther abortion in the CMS line occurred. Physiological and biochemical analyses of developing anthers and mitochondria revealed that over-accumulation of reactive oxygen species (ROS) in the SaNa-1A and deficiency in antioxidant enzyme system aggravated the oxidization of membrane lipids, resulting in malondialdehyde (MDA) accumulation in anthers. High MDA content in the CMS line was toxic to the cells. ROS accumulation in SaNa-1A also affected anther development. Abnormal structure and function of terminal oxidase, which participates in the electron transport chain of mitochondrial membrane, were observed and affected the activity of cytochrome c oxidase and F_1F_0-ATPase, which inhibited ATP biosynthesis. Proline deficiency in SaNa-1A also affected anther development. Few hybridization signals of programmed cell death (PCD) in tetrads of SaNa-1A were identified using TdT-mediated dUTP Nick-End Labeling assay. PCD was not obvious in tapetum cells of SaNa-1A until the unicellular stage. These results validated the cytological differences mentioned above, and proved that abnormal tapetum degradation and anther development in SaNa-1A were the main reasons for the anther abortion.

Keywords *Brassica napus* · Cytoplasmic male sterility · Tapetum · Programmed cell death · Energy metabolism

Introduction

Male sterility is an important accident in development of hermaphroditic plants (Wan et al. 2010). Cytoplasmic male sterility (CMS) has been defined as 'maternally' inherited deficiency in producing viable pollen, and is correlated with the gene distortion in mitochondria. Presently, it has been reported in ~150 higher plant species (Budar and Pelletier 2001; Li et al. 2017), and can be restored by nuclear fertility restoring (*Rf*) genes (Yamagishi and Bhat 2014). CMS as one of the ideal system for pollination controlling has greatly contributed to increase rapeseed production, and was classified into two types according to the origin of cytoplasm. The one type was derived from intergeneric hybridization or mutation during natural reproduction, including *pol* CMS, *nap* CMS and *Shan2A* CMS. The other type was caused by nucleus substitution or mitochondrial gene recombination during distant hybridization or protoplast fusion between the different species, including *Ogura* CMS and *tour* CMS (Shen et al. 2008; Leino et al. 2003). As reported, functional deficiency of sexual whorl in hermaphrodite species is related to programmed cell death (PCD), which is critical for development and release of anthers and pollen grains (Song et al. 2016; Varnier et al. 2005; Parish and Li 2010; Wilson

Communicated by Kinya Toriyama.

✉ Youping Wang
wangyp@yzu.edu.cn

[1] Jiangsu Provincial Key Laboratory of Crop Genetics and Physiology, Yangzhou University, Yangzhou 225009, China

[2] Guizhou Rapeseed Institute, Guizhou Academy of Agricultural Sciences, Guiyang 550008, China

et al. 2011). For example, PCD in tapetum is essential for late development of viable pollen, disruption or premature PCD in tapetum stage and other stages of anther development would result in microspore abortion and male sterility (Liu et al. 2018a; Ku et al. 2003; Li et al. 2006).

CMS is also associated with abnormal recombination of mitochondrial genome. Mitochondrion provides energy for cell activities through respiration, and it is also a major source of reactive oxygen species (ROS) that participates in oxidative eruption and triggers cell death (Green and Reed 1998; Liu et al. 2018b). However, excessive accumulation of superoxide (O_2^-), hydrogen peroxide (H_2O_2), and hydroxyl radical (·OH) could lead to cell death (Maxwell et al. 2002). Plants have developed various mechanisms (e.g., enzymatic and nonenzymatic) for ROS scavenging. Besides antioxidants such as ascorbate and glutathione, superoxide dismutase (SOD), ascorbate peroxidase, and catalase are well known as ROS-scavenging enzymes (Mostofa et al. 2015). As a widely used marker of oxidative lipid injury, and an abundant individual aldehydic lipid breakdown product, malondialdehyde (MDA) content varies in response to biotic and abiotic stress. In vivo, MDA and other aldehydes can alter proteins, DNA, RNA, and other biomolecules through Schiff base addition reactions, which are also toxic to cells (Esterbauer and Cheeseman 1990).

As mentioned above, the chimeric protein resulting from mitochondrial genome rearrangement is responsible for CMS in plants, which contains fragment of oxidative phosphorylation (OXPHOS) complex subunits (Hanson and Bentolila 2004). Hitherto, few researches on function of the chimeric proteins have been reported, but the mechanism of sterilizing factors is still unclear. For instance, the maize CMS-T URF13 protein (Rhoads et al. 2006) and Ogura CMS ORF138 (Duroc et al. 2006) resulted in a pore in inner membrane of mitochondrial. Protons could leak through the membrane pore, and result in uncoupling of respiratory chain and ATP synthase, leading to reduced ATP synthesis (Duroc et al. 2009). The interaction of sterilizing factor with respiratory chain has been reported in some CMS lines. The sunflower CMS is caused by the expression of ORF522, which interacts with the ATP synthase and affects its activity (Sabar et al. 2003). In the HL-CMS of rice, a chimeric protein ORFH79 interacts with a QCR10 subunit homologue of complex III (P61), which inhibits the activity of complex III, leads to reduced ATP level and increased ROS content (Wang et al. 2013).

The CMS line SaNa-1A containing 38 chromosomes was previously selected from the BC_3 progenies of *Brassica napus–Sinapis alba* somatic hybrids, using *B. napus* cv. 'Yangyou6' as recurrent parent (Wang et al. 2005). RNA-seq analysis was conducted on the abortion stage of floral buds from SaNa-1A CMS and the corresponding maintainer (SaNa-1B) (Du et al. 2016). In this study, a correlative structural approach using electron microscopy was employed to study anther development in SaNa-1A and SaNa-1B. In addition, the physiological indicators and PCD of sterile anthers were analyzed to characterize defects in degeneration or abnormalities in the tapetum.

Materials and methods

Plant materials

The novel CMS line (SaNa-1A) selected from progenies of somatic hybrids between *B. napus* and *S. alba*, and the maintainer line (SaNa-1B) was used in this study. Plant materials were cultivated in the experimental fields of Jiangsu Institute of Agricultural Science in the Lixiahe district (Yangzhou, Jiangsu Province). Different sizes of sterile and fertile anthers were fixed for cellular ultrastructure analysis.

Transmission electron microscopy (TEM)

For TEM, anthers at various developmental stages were prefixed in 0.1 N sodium phosphate buffer containing 2.5% glutaraldehyde (pH 7.2), and post-fixed in 2% OsO_4. Following ethanol dehydration, samples were embedded in epoxy resin. Ultrathin sections (60 nm) were obtained with a Leica UC6 ultramicrotome, and double stained with 2% (w/v) uranyl acetate and 2.6% (*w*/*v*) lead citrate aqueous solution. Images were recorded using a Philips Tecnai 12 transmission electron microscope (Wan et al. 2010).

TdT-mediated dUTP nick-end labeling (TUNEL) assay

Sections (10 μm) were washed with PBS (160 mM NaCl, 2.7 mM KCl, 8 mM Na_2HPO_4, and 1.5 mM KH_2PO_4) for 5 min and incubated in 20 μg/mL proteinase K in 100 mM Tris–HCl (pH 8.0) and 50 mM Na_2EDTA (100 μL per slide in a humid chamber). The sections were washed with PBS for 5 min and fixed with 4% (w/v) paraformaldehyde in PBS for 10 min. The sections were washed again in PBS for 5 min, and the 3′-OH ends of DNA were labeled with fluorescein 12-dUTP using the apoptosis detection system fluorescein (DeadEnd™ Fluorometric TUNEL System, Promega), according to the manufacturer's instructions (Balk and Leaver 2001). The fluorescent signal was viewed and photographed using an Eclipse Ni–U microscope (Nikon, Japan).

Isolation of mitochondria

All the extraction steps were performed at 4 °C. Anthers (200 g) were homogenized in 1000 mL buffer (0.5 M sucrose, 50 mM Tris–HCl, 10 mM EDTA, 1% bovine serum

albumin, 5 mmol/L β-mercaptoethanol, 1.5% polyvinylpyrrolidone, pH 7.5). The homogenate was filtered through a layer of cheesecloth and two layers of miracloth, and centrifuged at 3000 g for 15 min. The supernatant was then centrifuged at 17,000*g* for 15 min, and the pellet was re-suspended in buffer A [0.5 M sucrose, 50 mM Tris–HCl, 10 mM MgCl2, and 25 μg/mL DNase (Roche), pH 7.5] at a 5:1 (g/mL) ratio and kept at room temperature for 1 h. The suspension was then centrifuged at 18,000 g for 20 min, and the pellet was re-suspended in 30 mL of buffer B (0.6 M sucrose, 10 mM Tris–HCl, 20 mM EDTA, pH 7.5). The suspension was centrifuged again at 18,000*g* for 20 min. Finally, the pellet was re-suspended in the same buffer and layered onto a step gradient consisting of 1.45 M and 1.2 M sucrose solution containing 10 mM Tris–HCl and 20 mM EDTA (pH 7.5). The gradient was centrifuged at 72,000*g* for 90 min. Purified mitochondria were removed from the 1.45–1.2 M interphase, diluted with two volumes of buffer C (10 mM Tris–HCl, 20 mM EDTA, pH 7.5), and centrifuged at 18,000 g for 20 min (Chen et al. 2011).

Determination of H_2O_2, ATP, and MDA content

After staining the mitochondria with dihydrorhodamine 123 for 5 min, H_2O_2 generation was observed under a fluorescent microscope (Agilent Cary Eclipse, USA). H_2O_2 production in the isolated mitochondria was measured with a nonenzymatic assay according to Tiwari et al. (2002). The ATP content was measured using the luciferin–luciferase method (Zhang et al. 2014). ATP was dissolved in 5 mL of 25 mm HEPES buffer (pH 7.5), and luminescence from 200 μL sample was assayed in a chemiluminescence detector (Promega GloMax 20/20, USA) using luciferin–luciferase (ATP Assay Kit, Beyotime, China). The MDA content was measured spectrophotometrically at 532 nm, with the subtraction of non-specific absorption at 600 nm (Bradford 1976).

Analysis of antioxidant enzyme, COX, and F_1F_0-ATPase activities

SOD activity was assayed by measuring the inhibition of photochemical reduction of nitro blue tetrazolium, and peroxidase (POD) activity was determined by measuring the absorbance of the product of hydrogen peroxide and methyl catechol (Stewart and Bewley 1980). The activity of ETC complex V (F_0F_1-ATPase) was analyzed following the method described by Hu et al. (2010). Fresh mitochondria were obtained and sonicated to yield submitochondrial particles according to the protocol of the complex V assay kit (Genmed). Samples (10 μL) from the mitochondria (0.01 mg mitochondrial protein) were dissolved in 30 μL H_2O and 210 μL reaction substrate. The decrease in NADH was detected with a luminometer (Perkin Elmer) at 340 nm for 5 min, which was produced by coupling the production of ADP to the oxidation of NADH via pyruvate kinase and lactate dehydrogenase reactions. COX activity was analyzed as described by Ji et al. (2013), and the reaction mixture contained 50 mM phosphate buffer (pH 7.0), 10 μM reduced cytochrome c (reduced with 10 mM sodium ascorbate), and 10 μL of protein in a final volume of 1.5 mL.

Cytochemical detection of H_2O_2

H_2O_2 was visualized at the subcellular level using $CeCl_3$ for localization (Zhang et al. 2006). Electron-dense $CeCl_3$ deposits, viewed using TEM, were formed in the presence of H_2O_2. Anthers were dipped into freshly prepared 5 mM $CeCl_3$ in 50 mM MOPS (pH 7.2) for 1 h. The sections were then fixed in 1.25% (v/v) glutaraldehyde and 1.25% (v/v) paraformaldehyde in 50 mM sodium cacodylate buffer (pH 7.2) for 1 h. After fixation, the sections were washed twice for 10 min in the same buffer, post-fixed for 45 min in 1% (v/v) osmium tetroxide, dehydrated in a graded ethanol series (30–100%, v/v), and embedded in Epon–Araldite. After 12 h in pure resin followed by a change of fresh resin for 4 h, the samples were polymerized at 60 °C for 48 h. Blocks were sectioned (70–90 nm) on a microtome and mounted on uncoated copper grids. Sections were examined using a transmission electron microscope at an accelerating voltage of 75 kV.

Results

Ultrastructure of developing anthers in CMS and maintainer line

Previously, we found that SaNa-1A CMS line had shorter filaments, shriveled anthers with no pollen attached on the surface, and shriveled petals compared with SaNa-1B. Under microscope, the tapetum was not normally degraded at the unicellular stage of SaNa-1A, and the mature pollen could not be released (Du et al. 2016). To reveal the variations in subcellular level of anther development, we compared the ultrastructure of SaNa-1A and SaNa-1B, including different anther developmental stages, such as pollen mother cell (PMC) stage, tetrad stage, unicellular stage, and mature pollen stage.

At the PMC stage, cells in different layers of SaNa-1B anther were almost differentiated. The epidermis and endothecium cells were long and strip and had a large vacuole. The middle layer cells were prolate. All three layers were rich in endoplasmic reticulum, chloroplasts, and mitochondria (Fig. 1a). The tapetum cells were long and strip and had a large size with large nucleus, obvious nucleolus and nuclear membrane, rich in endoplasmic reticulum and

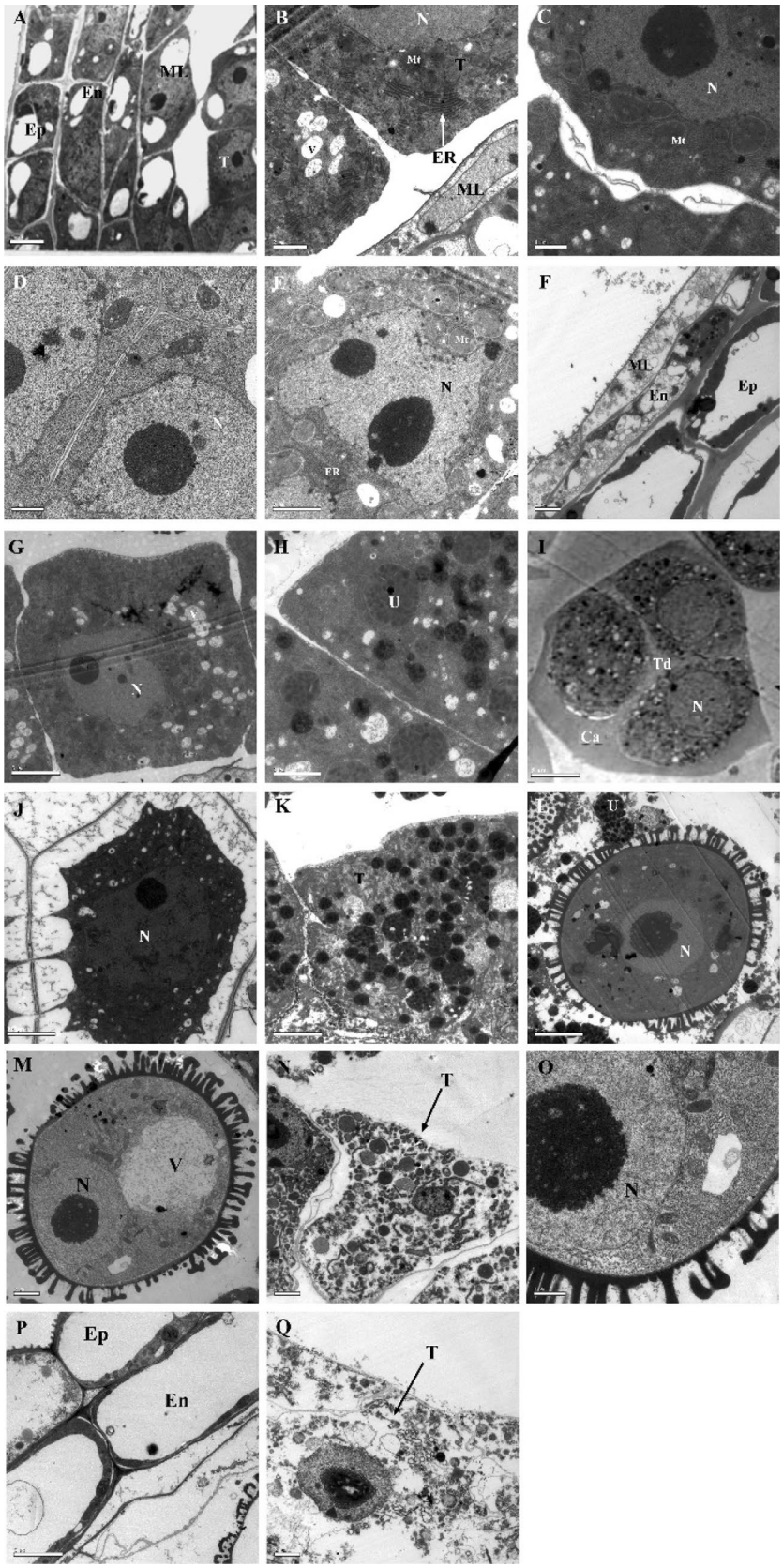

Fig. 1 Ultrastructure of maintainer line SaNa-1B at anther development stages. **a** Epidermis, endothecium, and middle layer at PMC stage (×1200), bar = 4 μm; **b** tapetum cells containing a small amount of vacuoles at PMC stage (×1200), bar = 2 μm; **c** tapetum cells containing abundant mitochondria, endoplasmic reticulum, and other organelles at PMC stage (×2200), bar = 1 μm; **d** pollen mother cells at PMC stage (×2200), bar = 1 μm; **e** meiosis of pollen mother cells (×1650), bar = 2 μm; **f** epidermis, endothecium and middle layer at Td stage (×900), bar = 2 μm; **g** tapetum cells containing a large number of vacuoles, lysosomes at Td stage (×1500), bar = 5 μm; **h** tapetum cells containing a lot of elaioplasts, tapetosomes at Td stage (×1650), bar = 2 μm; **i** microspore surrounded by callose (×2500), bar = 5 μm; **j** plasmodesmata between adjacent microspore (×3300), bar = 2 μm; **k** tapetum cells at Uni stage (×700), bar = 5 μm; **l** microspore surrounded by sporopollenin at early Uni stage (×700), bar = 5 μm; **m** late vacuolated pollen stage (×900), bar = 2 μm; **n** tapetum cells at MP stage (×900), bar = 2 μm; O: mature pollens (×2200), bar = 1 μm; **p** epidermis and endothecium at MP stage (×900), bar = 5 μm; **q** tapetum cells almost completely degraded at MP stage (×900), bar = 2 μm. *Ep* epidermis, *En* endothecium, *ML* middle layer, *T* tapetum, *N* nucleus, *Mt* mitochondria, *ER* endoplasmic reticulum, *V* vacuole, *E* elaioplasts, *Td* tetrad, *Ca* callose, *PMC* pollen mother cell, *Uni* unicellular, *MP* mature pollen

mitochondria (Fig. 1b, c). The PMCs had a polygon shape, large nucleus in the middle of cells, few vacuoles, obvious nucleolus, nuclear membrane and nucleoplasm, rich in endoplasmic reticulum and mitochondria. Moreover, we identified meiosis in some PMCs (Fig. 1d, e). At the tetrad stage, the epidermis, endothecium cell, and middle layer started to degrade (Fig. 1f). The cytoplasm of tapetum cells was rich in small vacuoles, lysosomes, spherical-shaped oleoplasts, tapetum corpuscles, and few starch granules (Fig. 1g, h). Tetrads were formed after meiosis of PMC, with oval shape, large and deeply dyed nucleus, condensed cytoplasm, and abundance of mitochondria and plastids. The tetrads were wrapped in callose, and low-density of electrons were lightly dyed (Fig. 1i, j). At the unicellular stage, the cell wall of tapetum started disappearing, and the cytoplasm was rich in tapetum corpuscles with electron deposits and deeply dyed oleoplast. Thus, the tapetum started to degrade (Fig. 1k). The callose surrounding the tetrad was gradually degraded by the callose enzyme secreted from tapetum, and microspores were separated and released into the anther locule. The round microspores were deposited with rich sporopollenin on the exine, which formed the columellae (Fig. 1l). At later unicellular stage, microspores grew rapidly, a large vacuole was formed, the nucleus was squeezed to one side, and the cytoplasm was condensed and rich in mitochondria. The thickness of microspore cell wall was gradually increased (Fig. 1m). The tapetum was completely disrupted at later unicellular stage, and the cytoplasmic organelles started to degrade (Fig. 1n). At the mature pollen stage, the bicellular pollen grain with nutritive and generative cells was formed after mitosis of mononuclear pollen. After another round of mitosis, the tricellular pollen grain was formed with two sperm cells and a nutritive cell. Meanwhile, the cytoplasmic activity of microspores with well-developed mitochondrial ridge was increased, and the vacuole started disappearing (Fig. 1o). The anther epidermis and endothecium were completely vacuolized, the middle layer disappeared (Fig. 1p), the tapetum was degraded, and the nucleus finally collapsed (Fig. 1q).

At the PMC stage, all the tissues were well developed in SaNA-1A, but the epidermis, endothecium, and middle layer cells did not have a regular shape and possessed larger vacuoles than those in SaNa-1B (Fig. 2a). The nuclear membranes of the tapetum in SaNa-1A were unclear, and its nucleolus was obviously smaller than that in SaNa-1B, indicating that tapetum development in SaNa-1A occurred later than that in SaNa-1B (Fig. 2b). The PMC in the CMS line was also smaller than SaNa-1B and contained vacuoles of different sizes, with the nucleus and cytoplasm squeezed to one side. Both the nucleus and kernel in SaNa-1A were smaller than those in SaNa-1B (Fig. 2c). This indicated that PMC development in CMS line was affected. Disruption of endoplasmic reticulum in PMC, disorder, and degradation of mitochondria was also observed in SaNa-1A. We found that the PMCs were severely vacuolized until the meiosis stage (Fig. 2d, e). At the tetrad stage, the tapetum had a large vacuole, deeply dyed cytoplasm, abundant lysosomes, and disrupted organelles and nuclear membrane (Fig. 2g). Meiosis was observed in some PMCs, but their inner structure was disrupted and the nuclear membrane was broken into discontinuous fragments (Fig. 2h). Abnormalities in outlook and inner structure of tetrads were observed in SaNa-1A, which were irregularly shaped and wrapped in thick callose. Microspores were identified with many vacuoles, the organelles were disrupted, and the endoplasmic reticulum, mitochondria, and some nucleolus disappeared (Fig. 2i, j). Anther epidermis and endothecium cells were completely vacuolized, and their middle layer gradually disappeared (Fig. 2k). At the unicellular stage, microspores in SaNa-1A were released from the tetrads, but they were severely vacuolized and their organelles were disrupted. The structures of the mitochondria and endoplasmic reticulum were incomplete, and the nucleus disappeared except for the small-sized nucleus that was squeezed in the middle of cells by the vacuole. Microspores were also surrounded by many sporopollenins (Fig. 2l, m). At the same time, the cell wall of tapetum disappeared, the cells started to degrade, and the oleoplasts and tapetum corpuscles appeared inside the tapetum (Fig. 2n). At later unicellular stage, microspore development was stopped. Although microspores were still surrounded with sporopollenins, they were degraded inside and inclusions were invisible (Fig. 2o). Moreover, the tapetum was filled with large vacuole, the cell structure did not collapse, although the nucleus and organelles were degrade (Fig. 2p). At the mature pollen stage, the tapetum of SaNa-1A was degraded, and numerous oleoplasts and tapetum corpuscles were released (Fig. 2q). Finally, the tapetum was completely degraded, and the microspores were enveloped in the degraded materials. Nothing was left inside the microspores, and they were surrounded with sporopollenins (Fig. 2r).

H_2O_2, MDA content, and antioxidant enzyme activities in the anthers of CMS and maintainer line

ROS accumulation in mitochondria is an important indicator of oxidative stress in cells, and oxygen-free radicals are signaling molecules of PCD in plant cells. Thus, excessive accumulation of ROS could severely cause cell damage and death. To determine if oxygen radicals were involved in pollen abortion of CMS, we analyzed the ROS content of anthers at different developmental stages. At the PMC stage, ROS was slightly higher in SaNa-1A than in SaNa-1B. At the unicellular stage, ROS greatly accumulated and reached the maximum value, which was three times of the ROS content in SaNa-1B. Afterward, ROS content was reduced in

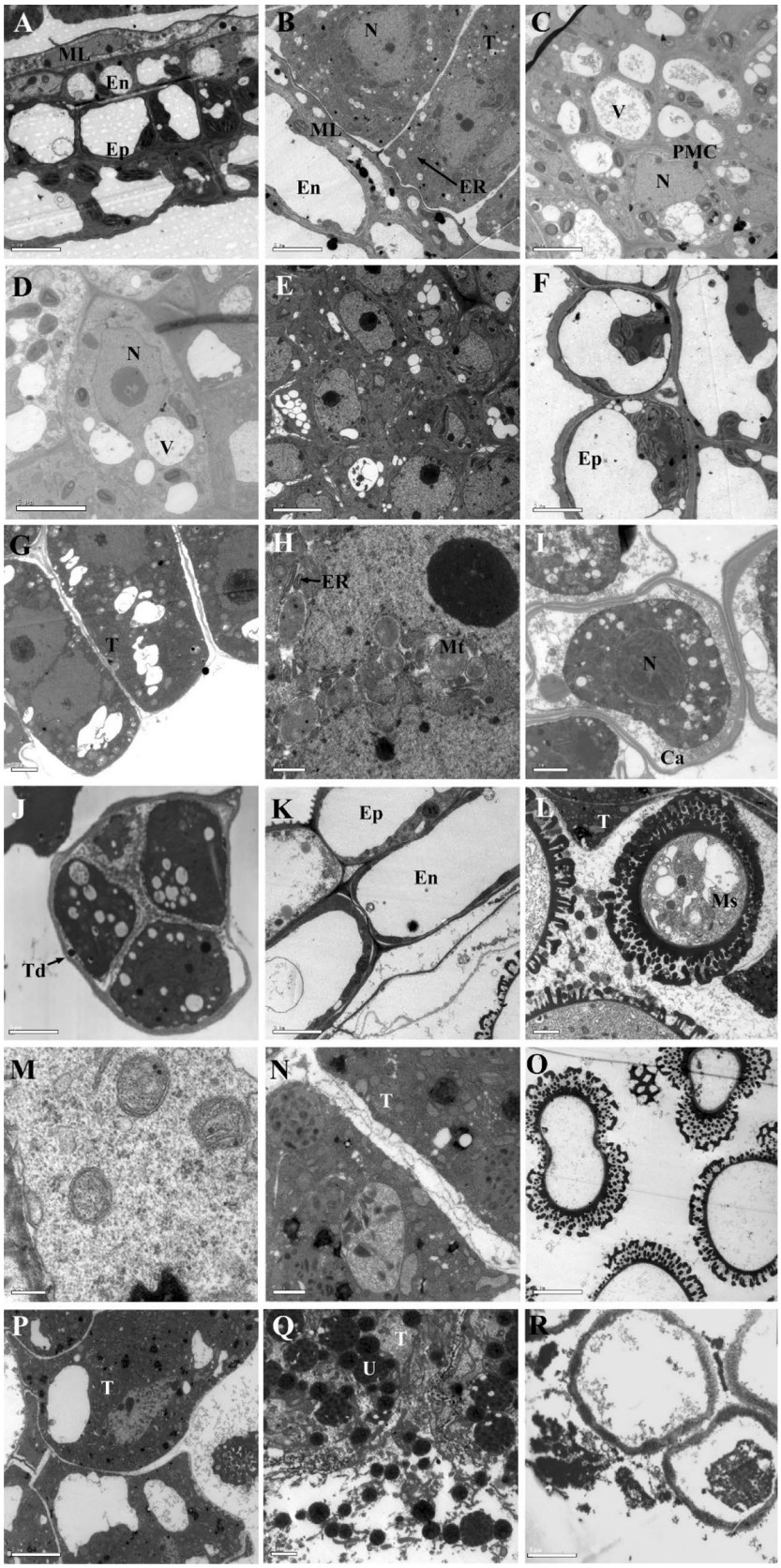

Fig. 2 Ultrastructure of sterile line SaNa-1A at anther development stage. **a** Epidermis, endothecium, middle layer cells with irregular shape at PMC stage (×1200), bar = 5 μm; **b** tapetum cells containing a lot of small vacuoles at PMC stage (×700), bar = 5 μm; **c** microsporocyte containing some large vacuoles at PMC stage (×700), bar = 5 μm; **d** microsporocyte containing abnormal organelles, and vacuolated seriously (×1200), bar = 5 μm; **e** microsporocyte at PMC stage (×700), bar = 5 μm; **f** epidermis at meiosis stage (×900), bar = 5 μm; **g** tapetum cells containing some large vacuole at Td stage (×900), bar = 2 μm; **h** microsporocyte occurring meiosis at Td stage (×1650), bar = 1 μm; **i** single microspore in the Td (×1200), bar = 2 μm; **j** Td structure (×900), bar = 5 μm; **k** epidermis and endothecium at Td stage (×700), bar = 5 μm; **l** microspore, incomplete mitochondria and endoplasmic reticulum structures at early Uni stage (×900), bar = 2 μm; **m** abnormal mitochondria of microspore at early Uni stage (×11,500), bar = 0.2 μm; **n** tapetum at early Uni stage (×1200), bar = 1 μm; **o** microspore without inclusion at late Uni stage (×700), bar = 5 μm; **p** tapetum at late Uni stage (×2200), bar = 5 μm; **q** degradation of tapetum (×1800), bar = 5 μm; R: aborted pollen (×1600), bar = 5 μm. *Ep* epidermis, *En* endothecium, *ML* middle layer, *T* Tapetum, *N* nucleus, *Mt* mitochondria, *ER* endoplasmic reticulum, *V* vacuole, *E* elaioplasts, *Td* tetrad, *Ca* callose, *PMC* pollen mother cell, *Uni* unicellular, *U* ubisch body

SaNa-1A, but it was still higher than that in SaNa-1B. We found that the ROS content in SaNa-1B was reduced with anther development (Fig. 3a).

MDA, the product of lipid peroxidation in cell membrane, serves as a parameter for determining the level of cell membrane injuries. MDA content was minimized at the tetrad stage of SaNa-1A, but it was relatively stable in SaNa-1B. MDA content in CMS line was significantly higher than that in SaNa-1B throughout anther development. This indicated that lipid peroxidation happened at the PMC stage of the CMS line, but it was relieved at the tetrad stage, and the mechanism did not last to the unicellular stage (Fig. 3b).

Antioxidant enzymes are important for clearing oxygen-free radicals and other metabolites that continuously accumulate and harm cell activity. They are helpful in balancing oxygen-free-radical content in cells, and protecting plant growth and development. At the microspore mother cell stage, SOD activity in SaNa-1B was slightly higher than that in SaNa-1A (Fig. 3c). At the tetrad and unicellular stages, SOD activity in SaNa-1B was significantly higher than that in SaNa-1A, and it was more than twice that of the PMC stage in SaNa-1B. With anther development, SOD activity in the CMS line was maximized at the tetrad stage, but it was significantly higher in SaNa-1B since tetrad stage. POD activity in the CMS line was significantly increased at the unicellular stage compared with that of the PMC and tetrad stages, which was also higher than the POD activity at the unicellular stage of SaNa-1B (Fig. 3d). These results indicated that active oxygen was greatly accumulated during anther development, and the maintainer line was able to clear active oxygen with improved SOD activity. Although the SOD activity was slightly increased in the CMS line with anther development, it was unable to maintain ROS balance. At later developmental stages of anthers, the increase of POD activity in CMS line might inhibited the biosynthesis of auxin and affected anther development.

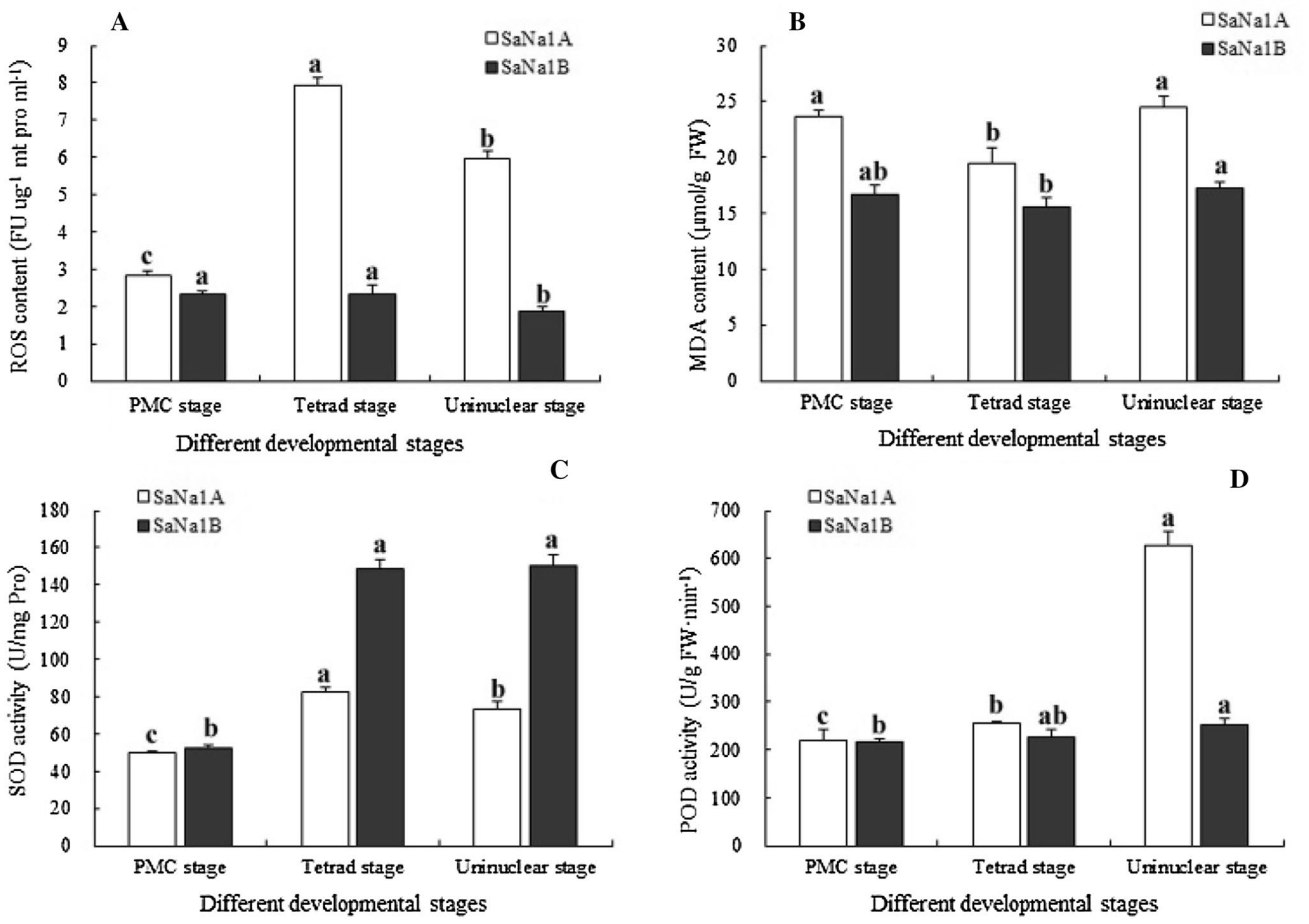

Fig. 3 H_2O_2 and MDA content, SOD and POD activity of the anthers at different developmental stages. **a** H_2O_2 content; **b** MDA content; **c** SOD activity; **d** POD activity. Different alphabets show significant difference of lines at $p < 0.05$ level

Cytochrome c Oxidase (COX) and F_1F_0-ATPase activities, ATP content in the anthers' mitochondria in the CMS and maintainer line

ATP is the most direct energy supplier for various biosynthesis and activities in cells. Variation in ATP content plays important roles in plant growth and development, and POD was reported to accompany ATP reduction (Tiwari et al. 2002). With anther development, ATP content was stable without significant changes in SaNa-1B. ATP content at the PMC stage of SaNa-1A resembled that of SaNa-1B, but it was significantly reduced afterward. At the unicellular stage, ATP content in SaNa-1A was 35% of that in SaNa-1B (Fig. 4a), indicating ATP deficiency, since the tetrad stage of CMS line might affect anther development.

F_1F_0-ATPase catalyzes ATP biosynthesis and hydrolyzes ATP into ADP. In this study, we found that F_1F_0-ATPase activity was maximized at the PMC stage of maintainer line and reduced at the tetrad and unicellular stages of SaNa-1B. F_1F_0-ATPase activity was significantly reduced at the tetrad and unicellular stages of SaNa-1A, which were also significantly lower than that in SaNa-1B. This finding indicated that stable F_1F_0-ATPase activity might be important for anther development in SaNa-1B (Fig. 4b), which is in agreement with the variation of ATP content in two rapeseed lines. Thus, we suspect the inhibition of F_1F_0-ATPase activity, since the tetrad stage of CMS line might affect ATP synthesis and anther development.

COX, an enzyme that functions at the end of the respiratory electron transfer chain, has been considered as a marker of mitochondria inner membrane of plants. Thus, it is important for energy metabolism in plants. We found that COX activity was maximized at the PMC stage of SaNa-1B and was significantly reduced at the unicellular stage. COX activity was significantly lower at the PMC and tetrad stages of CMS line compared with that in SaNa-1B (Fig. 4c), indicating that the respiratory pathways in CMS line were affected since the PMC stage.

Subcellular localization of H_2O_2 in the anthers of CMS and maintainer line

CMS has been reported to accompany ROS accumulation, and electron depositions from H_2O_2 and $CeCl_3$ reaction could be observed under TEM. Here, we compared the H_2O_2 content in epidermis and endothecium cells of CMS and maintainer lines' anthers. As shown in Fig. 5a, numerous electrons were deposited between the cell walls of epidermis cells in SaNa-1A, and few depositions were observed on the membrane and inner side of the chloroplast and mitochondria. At the tetrad and unicellular stages, electron depositions were increased in the CMS line, which were mostly found in the outer wall of cells (Fig. 5b, c). However, electron deposition was not observed throughout the anther development of SaNa-1B (Fig. 5d–f). This indicated H_2O_2 eruption at the PMC stage of CMS line, and was retained until the unicellular stage. Thus, ROS production greatly affected anther development, which was in agreement with the different ROS contents in two rapeseed lines.

TUNEL assay

At the PMC stage, positive hybridization signal of PCD was not observed in both CMS and maintainer lines (Fig. 6a, e). At the tetrad stage, PCD was identified in the tapetum of SaNa-1B (Fig. 6f, white arrowheads), and it was identified in the tetrads but not in the tapetum of CMS line (Fig. 6b). At the unicellular stage, PCD was increased in the tapetum of SaNa-1B (Fig. 6g), but few signals were identified in the CMS line (Fig. 6c). At the mature pollen stage, PCD events expanded to the external anthers of SaNa-1B, and they were identified in the epidermis cells (Fig. 6h). PCD was only observed in the middle of the anther locule and few tapetum cells (Fig. 6d). These results indicated that PCD occurred in tapetum cells of the maintainer line since the PMC stage, it increased and extended to the outside layer of anthers, which was necessary for pollen release. From the tetrad to unicellular stage, PCD in the CMS line was much less compared

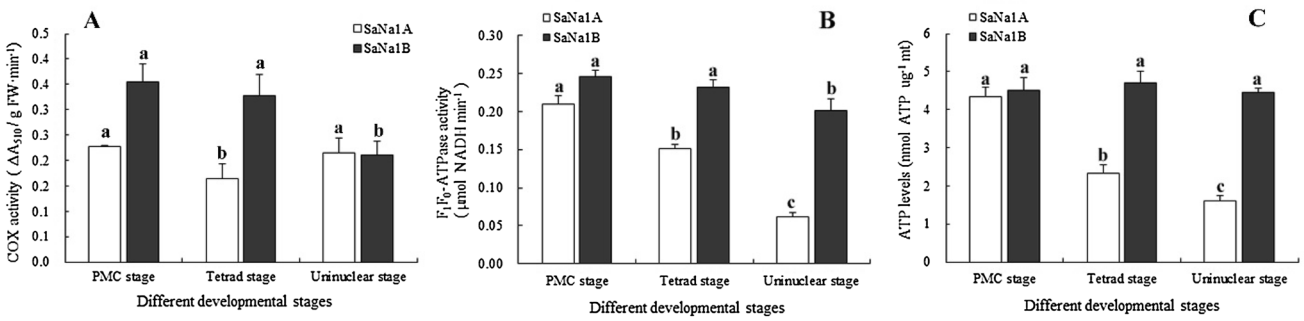

Fig. 4 ATP levels, COX, and F_1F_0-ATPase activity of the anthers' mitochondrion at different developmental stages. **a** COX activity; **b** F_1F_0-ATPase activity; **c** ATP levels. Different alphabets show significant difference of lines at $p < 0.05$ level

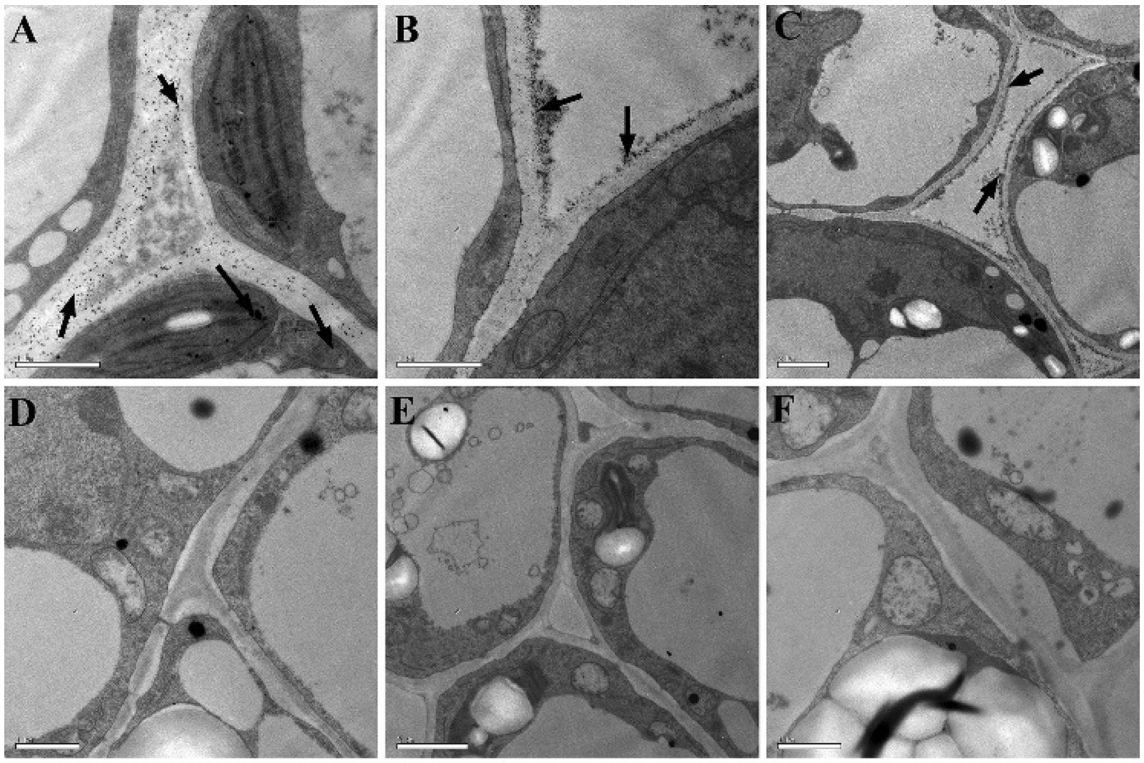

Fig. 5 Sites of electron-dense deposits of the epidermic cells or endothecium cells at different developmental stages. **a** CMS line SaNa-1A of PMC stage, bar = 1 μm; **b** CMS line SaNa-1A of tetrad stage, bar = 1 μm; **c** CMS line SaNa-1A of unicellular stage, bar = 2 μm; **d** maintainer line SaNa-1B of PMC stage, bar = 1 μm; **e** maintainer line SaNa-1B of tetrad stage, bar = 2 μm; **f** maintainer line SaNa-1B of unicellular stage, bar = 1 μm. The black arrows indicated the electron-dense deposits after Ce-H_2O_2 reaction

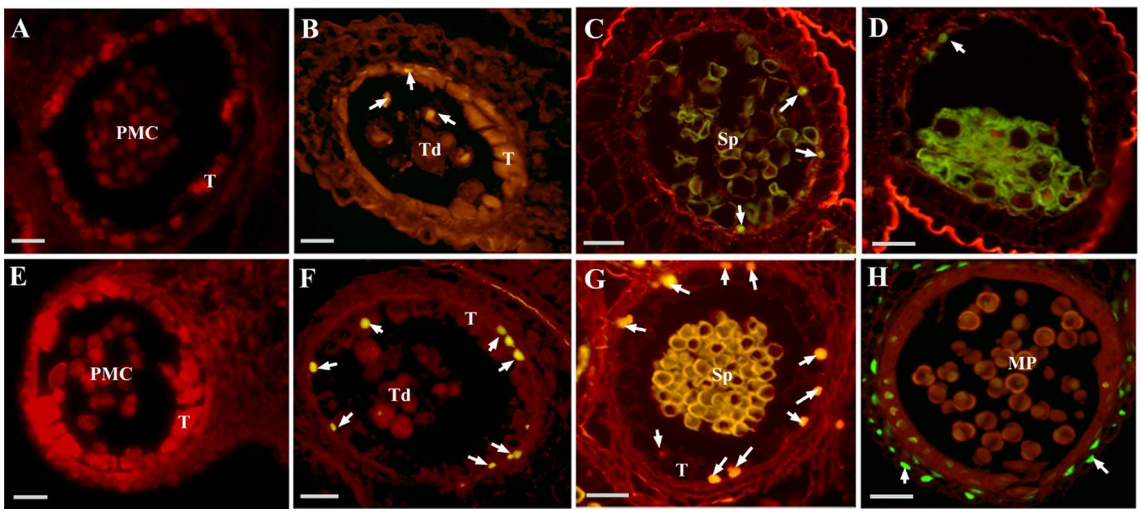

Fig. 6 DNA break detection in anther of SaNa-1A and SaNa-1B using TUNEL assay. **a–d** CMS line SaNa-1A; **e–h** maintainer line SaNa-1B; **a, e** PMC stage; **b, f** tetrad stage; **c, g** unicellular stage; **d, h** mature pollen stage. The white arrows indicated the signal of green or yellow–green fluorescent hybridization. *PMC* microsporocyte, *Td* tetrad, *Sp* microspore, *T* tapetum, *MP* mature pollen. Bar = 50 nm

with that in SaNa-1B, indicating that PCD was delayed in the CMS line and microspore development was hindered since the tetrad stage. In general, the different PCD events reflected the cytological difference between the CMS and maintainer lines, and confirmed that the abnormality in tapetum apoptosis and degradation was related to the sterility of SaNa-1A.

Discussion

Anther abortion mechanism in *B. napus* CMS line SaNa-1A

The ultrastructure of anther development in rapeseed CMS line has been broadly reported, and anther abortion and tapetum degradation have been correlated with sterility (Polowick and Sawhney 1990; Gonzalez-Melendi et al. 2008; Dun et al. 2011). Tsvetova and Elkonin (2003) reported two mechanisms of anther abortion related to tapetum development. First, early degradation of tapetum hindered the secretion of callose enzyme for microspore release from tetrads. The degraded tapetum invaded into the anther locule and caused abortion. Second, inflated tapetum cells squeezed microspores and caused anther abortion. Taylor et al. (1998) found that anther abortion in *Arabidopsis* CMS line *ms7* was caused by advanced degradation of tapetum cells. Balk and Leaver (2001) reported that sunflower PET1-CMS was caused by early PCD in tapetum. Gonzalez-Melendiet et al. (2008) found that Ogu-INRA CMS was also caused by the early degradation of tapetum cells. Contrarily, Polowick and Sawhney (1990) found that *Ogu* CMS of *B. napus* was due to the delay of tapetum degradation. Yang et al. (2008) reported the same mechanism in sesame CMS line. Vizcay-Barrena and Wilson (2006) compared wild type and *ms1* mutant in *Arabidopsis*, and found that PCD occurred in the tapetum since mitosis of microspores in wild type, whereas PCD was not normally observed in the mutant. In the present study, we found that the degradation of tapetum was also delayed, and the callose enzyme was not normally secreted from the tetrads. Thus, microspores were disabled because of nutrient deficiency and were not normally released.

Moreover, the mitochondrion is the center of oxidation–reduction reactions and respiration and is thus an important organelle for energy metabolism. The number of mitochondria and attached functional proteins was greatly increased with anther development (Linke and Börner 2005; Chase 2007). Thus, CMS is closely correlated with degradation and functional disorder of the mitochondria. In the present study, abnormality of the organelles, such as mitochondria, endoplasmic reticulum, and nucleolus, was observed since meiosis of PMCs in the CMS line. Thus, we suspected that the disruption and degradation of organelles resulted in the functional disorder in the CMS line, which affected anther development.

Reactive oxygen metabolism in mitochondria of the CMS line

The mitochondrion is the main site for ROS generation in higher plants. We found that ROS content in isolated mitochondria of SaNa-1A was slightly higher than that in SaNa-1B before microspore abortion, indicating that the deficiency of ROS clearance happened at the beginning of anther development in SaNa-1A. ROS content of the mitochondria significantly increased and maximized at the tetrad stage of CMS line. Similar variation in ROS content was also reported in the mitochondria of HL rice and cotton CMS lines (Li et al. 2004; Wan et al. 2007; Jiang et al. 2007). Subcellular localization of H_2O_2 also revealed ROS eruption at the PMC stage of SaNa-1A, and Cs-H_2O_2 complexes accumulated at the cell wall, mitochondria, and chloroplast, which were maximized at the tetrad stage. These observations agreed with the different ROS accumulations in two rapeseed lines.

SOD activity was significantly increased with microspore abortion in SaNa-1A, indicating that ROS accumulation positively induced SOD activity. However, the limited SOD activity in the CMS line was unable to clear the accumulated ROS; thus, ROS content was maximized at the tetrad stage of SaNa-1A. POD content in SaNa-1A was significantly increased at the unicellular stage of SaNa-1B, but it was stable in the CMS line. POD might be related to ROS clearance and balance of IAA content. The increased POD content in CMS line might accelerate IAA decomposition and cause nutrient deficiency in microspore development. MDA accumulation is related to biotic and abiotic stresses in plants (Esterbauer and Cheeseman 1990). We found that MDA content in isolated mitochondria was higher at different anther developmental stages of SaNa-1A than that of SaNa-1B, and the variation of MDA content in two rapeseed lines was consistent with the different ROS accumulation. This finding also indicated that excessive ROS accumulation in the CMS line would cause MDA accumulation, cell injury, and anther abortion.

Functional disorder of terminal oxidase of respiratory electron transfer chain in CMS line

COX is a terminal oxidase of the respiratory electron transfer chain, which plays important roles in aerobic organisms. COX deficiency can affect ATP biosynthesis and anther development (Rich and Bonner 1978). In the present study, COX activity at the PMC stage of the CMS line was significantly lower than that in SaNa-1B, indicating that COX deficiency inhibited the respiratory pathway. Ji et al. (2013) found that COX activity at different anther developmental stages of pepper CMS line was lower than that in the maintainer line. Consistent with the findings of Jiang et al. (2007), we found that COX activity was improved after microspore abortion in SaNa-1A, but it was not significantly different to that of the maintainer line.

Pollen development is an energy-consuming process, and dehydration resembling drought stress is necessary for the

development of mature pollens (McCormick 2004; Pastore et al. 2007). ATP biosynthesis in anthers of higher plants is catalyzed by F_1F_0-ATPase (Li et al. 2010). In the Boro II type of rice mitochondria, Wang et al. (2006) reported that a toxic protein encoded by *orf79*, which was downstream of *atp6*, affected anther development. Zhang et al. (2007) found that the CMS-related gene *atp6-orfH79* encoded a competitive protein of ATP6, and affected the structure and function of F_1F_0-ATPase. In *Arabidopsis*, mutation of *MGP1*, encoding the F_Ad subunit of F_1F_0-ATPase, affected the mitochondrial structure during pollen mutation and increased the hydrolysis activity of F_1F_0-ATPase (Li et al. 2010). Yang et al. (2008) identified that the expressional changes on *atpA*, which was downstream of *orf220*, reduced ATP biosynthesis in the mitochondria and resulted in anther abortion in the CMS line of rapeseed. In general, mutation of genes encoding F_1F_0-ATPase subunits affects mitochondrial function and induces disorder in ATP synthesis and hydrolysis.

In this study, ATP content in mitochondria of CMS and maintainer lines was similar at the early developmental stage of anthers, but it was reduced at later developmental stages of SaNa-1A. ATP content in SaNa-1B was much stable than that in the CMS line, indicating that ATP deficiency might be responsible for anther abortion. We also found that ATP content was positively correlated with F_1F_0-ATPase activity.

ROS-mediated PCD and anther abortion

PCD in plants was regulated by genes and characterized by apoptosis in cell structure, such as cell shrinking, karyopyknosis, chromosome condensation, and DNA fragmentation. In general, a lag phase existed between DNA fragmentation and cell structure abnormality. Li et al. (2004) reported that DNA fragmentation in tapetum started with meiosis in the rice CMS line, and cell structure abnormality in tapetum was observed at later microspore stage. Microspore abortion in the CMS line of sunflower and rice was mainly due to the abnormal PCD events in tapetum (Ku et al. 2003; Balk and Leaver 2001). Shi et al. (2009) revealed that advanced PCD in tapetum of rice photosensitive genic male sterile line 58S was the main cause of anther abortion. Wan et al. (2010) reported that abnormal and advanced PCD in tapetum of *B. napus* recessive genic male CMS line 9012A was related to anther abortion, indicating that PCD in tapetum was closely related to male sterility. In the present study, the differences of PCD in tapetum were observed since the tetrad stage of CMS and maintainer lines, which indicating that tapetum was not normally degraded at the tetrad stage of SaNa-1A.

ROS is an important signal transduction mechanism in regulating and transferring PCD signals. Excessive accumulation of ROS could induce membrane peroxidation and PCD (Hoeberichts and Woltering 2003; Mittler et al. 2004). In this study, ROS accumulated since the PMC

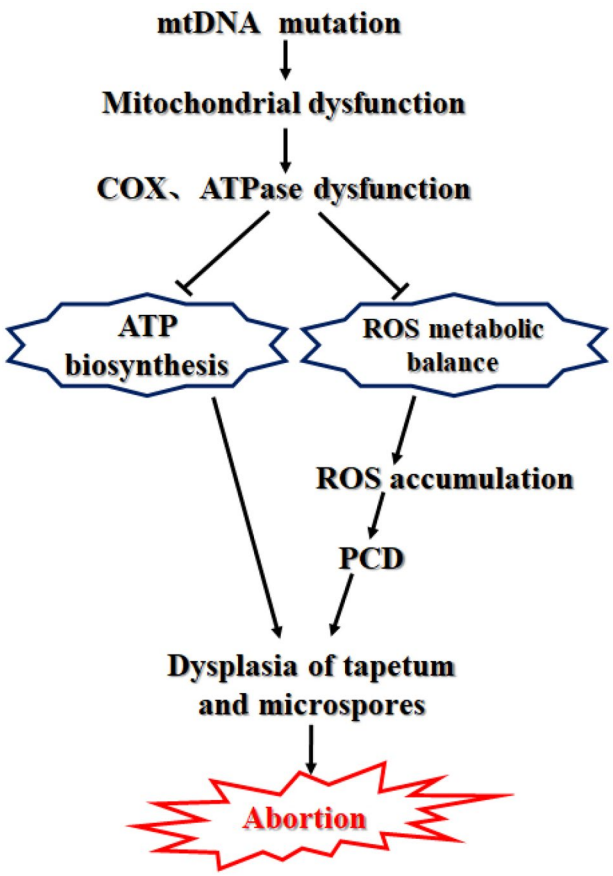

Fig. 7 Proposed model for physiological mechanism of CMS line SaNa-1A

stage of SaNa-1A. Abnormality in antioxidant enzyme system was observed afterward, and PCD was identified in the microspores at the tetrad stage. Meanwhile, the structure and function of cells in CMS anthers became abnormal. All the differences indicated that ROS accumulation and PCD occurred at the same time, and ROS was an important signal molecule regulating antioxidant enzyme activity and it also involved in the PCD of microspores. ROS stress in SaNa-1A was observed since the PMC to unicellular stage, which was long enough to affect mitochondrial function and gene expression, and finally influence microspore development. Thus, we suspected that oxidative stress is the main reason of anther abortion in the CMS line.

In the present study, we compared the ultra-microstructure of anthers between a CMS line (SaNa-1A) from *B. napus–S. alba* somatic hybrids and a maintainer line (SaNa-1B). We found that abnormal PMC development and delay of tapetum degradation were the main reasons for anther abortion in SaNa-1A. Physiological and biochemical analyses indicated that the high ROS content in the CMS line might improve the activity of antioxidant enzyme system,

whereas the reduced SOD activity and increased POD activity might inhibit anther development. Variations in mitochondria structure affected the structure and function of the terminal oxidase of the respiratory electron transfer chain, and ATP biosynthesis was affected by the inhibition of F_1F_0-ATPase activity regulated by COX activity. Identification of DNA fragmentation revealed that ROS accumulation induced PCD at the tetrad stage of microspores, and PCD in tapetum was abnormal in the CMS line, which delayed the nutrient supply for microspores and finally caused anther abortion. Previously, the RNA-seq analysis indicated that genes participating in carbon metabolism, tricarboxylic acid cycle, oxidative phosphorylation, oxidation–reduction system, pentatricopeptide repeat, and anther development were downregulated significantly in the SaNa-1A CMS line (Du et al. 2016). In general, all the above-mentioned differences between CMS and maintainer lines were consistent with the expressional difference from RNA-seq analysis. We provided a hypothetical model for the abortion mechanism of SaNa-1A (Fig. 7).

Author contribution statement YW conceived and designed the study. KD, YX, QL, and JJ participated in the experiments. JW, YF, and YX analyzed data and wrote the manuscript. All authors drafted the manuscript and approved the final manuscript.

Acknowledgements This research was funded by the National Natural Science Foundation of China (31330057, 31571699, 31771824), the National Key Research and Development Program of China (2016YFD0102000, 2016YFD0101000), the National Key Basic Research Program of China (2015CB150201), the Natural Science Foundation of Jiangsu Province (BE2018356, BK20180101), and the Priority Academic Program Development of Jiangsu Higher Education Institutions.

Compliance with ethical standards

Conflict of interest The authors declare no conflict of interest.

References

Balk J, Leaver CJ (2001) The PET1-CMS mitochondrial mutation in sunflower is associated with premature programmed cell death and cytochrome c release. Plant Cell 13:1803–1818. https://doi.org/10.1105/TPC.010116

Bradford MM (1976) A rapid and sensitive method for the quantitation of microgram quantities of protein utilizing the principle of protein-dye binding. Anal Biochem 72:248–254. https://doi.org/10.1016/0003-2697(76)90527-3

Budar F, Pelletier G (2001) Male sterility in plants: occurrence, determinism, significance and use. C R Acad Sci III 324:543–550. https://doi.org/10.1016/S0764-4469(01)01324-5

Chase CD (2007) Cytoplasmic male sterility: a window to the world of plant mitochondrial-nuclear interactions. Trends Genet 23:81–90. https://doi.org/10.1016/j.tig.2006.12.004

Chen JM, Guan RZ, Chang SX, Du TQ, Zhang HS, Xing H (2011) Substoichiometrically different mitotypes coexist in mitochondrial genomes of *Brassica napus* L. Plos One 6:260–260. https://doi.org/10.1371/journal.pone.0017662

Du K, Liu QE, Wu XY, Jiang JJ, Wu J, Fang YJ, Li AM, Wang YP (2016) Morphological structure and Ttranscriptome comparison of the cytoplasmic male sterility line in *Brassica napus* (SaNa-1A) derived from somatic hybridization and its maintainer line SaNa-1B. Front Plant Sci 7:1313. https://doi.org/10.3389/fpls.2016.01313

Dun XL, Zhou ZF, Xia SQ, Wen J, Yi B, Shen JX, Ma CZ, Tu JX, Fu TD (2011) BnaC.Tic40, a plastid inner membrane translocon originating from *Brassica oleracea*, is essential for tapetal function and microspore development in *Brassica napus*. Plant J 68:532–545. https://doi.org/10.1111/j.1365-313X.2011.04708.x

Duroc Y, Gaillard C, Hiard S, Tinchant C, Berthomé R, Pelletier G, Budar F (2006) Nuclear expression of a cytoplasmic male sterility gene modifies mitochondrial morphology in yeast and plant cells. Plant Sci 170:755–767. https://doi.org/10.1016/j.plantsci.2005.11.008

Duroc Y, Hiard S, Vrielynck N, Ragu S, Budar F (2009) The Ogura sterility-inducing protein forms a large complex without interfering with the oxidative phosphorylation components in rapeseed mitochondria. Plant Mol Biol 70:123–137. https://doi.org/10.1007/s11103-009-9461-6

Esterbauer H, Cheeseman KH (1990) Determination of aldehydic lipid peroxidation products: malonaldehyde and 4-hydroxynonenal. Method Enzymol 186:407–421. https://doi.org/10.1016/0076-6879(90)86134-H

Gonzalez-Melendi P, Uyttewaal M, Morcillo CN, Hernández Mora JR, Fajardo S, Budar F, Lucas MM (2008) A light and electron microscopy analysis of the events leading to male sterility in Ogu-INRA CMS of rapeseed (*Brassica napus*). J Exp Bot 59:827–838. https://doi.org/10.1093/jxb/erm365

Green DR, Reed JC (1998) Mitochondria and Apoptosis. Science 281:1309–1312

Hanson MR, Bentolila S (2004) Interactions of mitochondrial and nuclear genes that affect male gametophyte development. Plant Cell 16:154–169. https://doi.org/10.1105/tpc.015966

Hoeberichts FA, Woltering EJ (2003) Multiple mediators of plant programmed cell death: Interplay of conserved cell death mechanisms and plant-specific regulators. Bioessays 25:47–57. https://doi.org/10.1002/bies.10175

Hu CF, Sun QP, Peng XJ, Huang Q, Wang MF, Li SQ, Zhu YG (2010) Flow cytometric analysis of mitochondrial populations in HL-CMS systems of rice under H_2O_2 stress. Protoplasma 241:91–98. https://doi.org/10.1007/s00709-009-0101-4

Ji JJ, Huang W, Yin CC, Gong ZH (2013) Mitochondrial cytochrome c oxidase and F_1F_0-ATPase dysfunction in peppers (*Capsicum annuum* L.) with cytoplasmic male sterility and its association with *orf507* and *Ψatp6-2* genes. Int J Mol Sci 14:1050–1068. https://doi.org/10.3390/ijms14011050

Jiang PD, Zhang XQ, Zhu YG, Zhu W, Xie HY, Wang XD (2007) Metabolism of reactive oxygen species in cotton cytoplasmic male sterility and its restoration. Plant Cell Rep 26:1627–1634. https://doi.org/10.1007/s00299-007-0351-6

Ku S, Yoon H, Suh HS, Chung YY (2003) Male-sterility of thermosensitive genic male-sterile rice is associated with premature programmed cell death of the tapetum. Planta 217:559–565. https://doi.org/10.1007/s00425-003-1030-7

Leino M, Teixeira R, Landgren M, Glimelius K (2003) *Brassica napus* lines with rearranged Arabidopsis mitochondria display CMS and a range of developmental aberrations. Theor

Appl Genet 106:1156–1163. https://doi.org/10.1007/s00122-002-1167-y

Li SQ, Wan CX, Kong J, Zhang ZJ, Li YS, Zhu YG (2004) Programmed cell death during microgenesis in a Honglian CMS line of rice correlated with oxidative stress in mitochondria. Funct Plant Biol 31:369–376. https://doi.org/10.1071/FP03224

Li N, Zhang DS, Liu HS, Yin CS, Li XX, Liang WQ et al (2006) The rice tapetum degeneration retardation gene is required for tapetum degradation and anther development. Plant Cell 18:2999–3014. https://doi.org/10.1105/tpc.106.044107

Li WQ, Zhang XQ, Xia C, Deng Y, Ye D (2010) Male gametophyte defective 1, encoding the F_Ad subunit of mitochondrial F_1F_0-ATP synthase, is essential for pollen formation in *Arabidopsis thaliana*. Plant Cell Physiol 51:923–935. https://doi.org/10.1093/pcp/pcq066

Li YW, Ding XL, Wang X, He TT, Zhang H, Yang LS et al (2017) Genome-wide comparative analysis of DNA methylation between soybean cytoplasmic male-CMS line NJCMS5A and its maintainer NJCMS5B. BMC Genom 18:596. https://doi.org/10.1186/s12864-017-3962-5

Linke B, Börner T (2005) Mitochondrial effects on flower and pollen development. Mitochondrion 5:389–402. https://doi.org/10.1016/j.mito.2005.10.001

Liu ZH, Shi XY, Li S, Hu G, Zhang LL, Song XY (2018a) Tapetal-delayed programmed cell death (PCD) and oxidative stress-induced male sterility of *Aegilops uniaristata* cytoplasm in wheat. Int J Mol Sci 19:1708. https://doi.org/10.3390/ijms19061708

Liu ZH, Shi XY, Li S, Zhang LL, Song XY (2018b) Oxidative stress and aberrant programmed cell death are associated with pollen abortion in isonuclear alloplasmic male-sterile wheat. Front Plant Sci 9:595. https://doi.org/10.3389/fpls.2018.00595

Maxwell DP, Nickels R, McIntosh L (2002) Evidence of mitochondrial involvement in the transduction of signals required for the induction of genes associated with pathogen attack and senescence. Plant J 29:269–279. https://doi.org/10.1046/j.1365-313X.2002.01216.x

McCormick S (2004) Control of male gametophyte development. Plant Cell 116:S142–S153. https://doi.org/10.1105/tpc.016659

Mittler R, Vanderauwera S, Gollery M, Van Breusegem F (2004) Reactive oxygen gene network of plants. Trends Plant Sci 9:490–498. https://doi.org/10.1016/j.tplants.2004.08.009

Mostofa MG, Hossain MA, Fujita M, Tran LS (2015) Physiological and biochemical mechanisms associated with trehalose-induced copper-stress tolerance in rice. Sci Rep UK 5:11433. https://doi.org/10.1038/srep11433

Parish RW, Li SF (2010) Death of a tapetum: A programme of developmental altruism. Plant Sci 178:73–89. https://doi.org/10.1016/j.plantsci.2009.11.001

Pastore D, Trono D, Laus MN, Di Fonzo ND, Flagella Z (2007) Possible plant mitochondria involvement in cell adaptation to drought stress. A case study: durum wheat mitochondria. J Exp Bot 58:195–210. https://doi.org/10.1093/jxb/erl273

Polowick PL, Sawhney VK (1990) Microsporogenesis in a normal line and in the ogu cytoplasmic male-sterile line of *Brassica napus*. I. The influence of high temperatures. Sex Plant Reprod 3:263–276. https://doi.org/10.1007/BF00194567

Rhoads DM, Umbach AL, Subbaiah CC, Siedow JN (2006) Mitochondrial reactive oxygen species. Contribution to oxidative stress and interorganellar signaling. Plant Physiol 141:357–366. https://doi.org/10.1104/pp.106.079129

Rich PR, Bonner WD (1978) The sites of superoxide anion generation in higher plant mitochondria. Arch Biochem Biophys 188:206–213. https://doi.org/10.1016/0003-9861(78)90373-9

Sabar M, Gagliardi D, Balk J, Leaver CJ (2003) ORFB is a subunit of F_1F_0-ATP synthase: insight into the basis of cytoplasmic male sterility in sunflower. EMBO Rep 4:381–386. https://doi.org/10.1038/sj.embor.embor800

Shen JX, Wang HZ, Fu TD, Tian BM (2008) Cytoplasmic male sterility with self-incompatibility, a novel approach to utilizing heterosis in rapeseed (*Brassica napus* L.). Euphytica 162:109–115. https://doi.org/10.1007/s10681-007-9606-0

Shi YL, Zhao S, Yao JL (2009) Premature tapetum degeneration: a major cause of abortive pollen development in photoperiod sensitive genic male sterility in rice. J Integr Plant Biol 51:774–781. https://doi.org/10.1111/j.1744-7909.2009.00849.x

Song LP, Zhou ZF, Tang S, Zhang ZQ, Xia SQ, Qin MM et al (2016) Ectopic expression of BnaC.CP20.1 results in premature tapetal programmed cell death in Arabidopsis. Plant Cell Physiol 57:1972–1984. https://doi.org/10.1093/pcp/pcw119

Stewart RRC, Bewley JD (1980) Lipid peroxidation associated with accelerated aging of soybean axes. Plant Physiol 65:245–248. https://doi.org/10.1104/pp.65.2.245

Taylor PE, Glover JA, Lavithis M, Craig S, Singh MB, Knox RB, Dennis ES, Chaudhury AM (1998) Genetic control of male fertility in *Arabidopsis thaliana*: structural analyses of postmeiotic developmental mutants. Planta 205:492–505. https://doi.org/10.1007/s004250050348

Tiwari BS, Belenghi B, Levine A (2002) Oxidative stress increased respiration and generation of reactive oxygen species, resulting in ATP depletion, opening of mitochondrial permeability transition, and programmed cell death. Plant Physiol 128:1271–1281. https://doi.org/10.1104/pp.010999

Tsvetova MI, Elkonin LA (2003) Cytological investigation of male sterility in sorghum caused by a dominant mutation (*Mstc*) derived from tissue culture. Sex Plant Reprod 16:43–49. https://doi.org/10.1007/s00497-003-0172-x

Varnier AL, Mazeyrat-Gourbeyre F, Sangwan RS, Clément C (2005) Programmed cell death progressively models the development of anther sporophytic tissues from the tapetum and is triggered in pollen grains during maturation. J Struct Biol 152:118–128. https://doi.org/10.1016/j.jsb.2005.07.011

Vizcay-Barrena G, Wilson ZA (2006) Altered tapetal PCD and pollen wall development in the *Arabidopsis ms1* mutant. J Exp Bot 57:2709–2717. https://doi.org/10.1093/jxb/erl032

Wan CX, Li SQ, Wen L, Kong J, Wang K, Zhu YG (2007) Damage of oxidative stress on mitochondria during microspores development in Honglian CMS line of rice. Plant Cell Rep 26:373–382. https://doi.org/10.1007/s00299-006-0234-2

Wan LL, Xia XY, Hong DF, Li J, Yang GS (2010) Abnormal vacuolization of the tapetum during the tetrad stage is associated with male sterility in the recessive genic male sterile *Brassica napus* L. line 9012A. J Plant Biol 53:121–133. https://doi.org/10.1007/s12374-009-9095-x

Wang YP, Sonntag K, Rudloff E, Chen JM (2005) Intergeneric somatic hybridization between *Brassica napus* L. and *Sinapis alba* L. J Integr Plant Biol 47:84–91. https://doi.org/10.1111/j.1744-7909.2005.00009.x

Wang ZH, Zou YJ, Li XY, Zhang QY, Chen LT, Wu H et al (2006) Cytoplasmic male sterility of rice with Boro II cytoplasm is caused by a cytotoxic peptide and is restored by two related PPR motif genes via distinct modes of mRNA silencing. Plant Cell 18:676–687. https://doi.org/10.1105/tpc.105.038240

Wang K, Gao F, Ji YX, Liu Y, Dan ZW, Yang PF, Zhu YG, Li SQ (2013) ORFH79 impairs mitochondrial function via interaction with a subunit of electron transport chain complex III in Honglian cytoplasmic male sterile rice. New Phytol 198:408–418. https://doi.org/10.1111/nph.12180

Wilson ZA, Song J, Taylor B, Yang CY (2011) The final split: the regulation of anther dehiscence. J Exp Bot 62:1633–1649. https://doi.org/10.1093/jxb/err014

Yamagishi H, Bhat SR (2014) Cytoplasmic male sterility in Brassicaceae crops. Breed Sci 64:38–47. https://doi.org/10.1270/jsbbs.64.38

Yang XL, Zhang HY, Guo WZ, Zheng YZ, Miao HW, Wei LB, Zhang TZ (2008) Ultrastructure in microspore abortion of genic male sterile line in sesame (*Sesamum indicum* L.). Acta Agro Sin 34:1894–1900. https://doi.org/10.1016/S1875-2780(09)60014-6

Zhang AY, Jiang MY, Zhang JH, Tan MP, Hu XL (2006) Mitogen-activated protein kinase is involved in abscisic acid-induced antioxidant defense and acts downstream of reactive oxygen species production in leaves of maize plants. Plant Physiol 141:475–487. https://doi.org/10.1104/pp.105.075416

Zhang H, Li SQ, Yi P, Wan CX, Chen ZY, Zhu YG (2007) A Honglian CMS line of rice displays aberrant F_0 of F_1F_0-ATPase. Plant Cell Rep 26:1065–1071. https://doi.org/10.1007/s00299-006-0293-4

Zhang XL, Zuo XX, Yang B, Li ZR, Xue YC, Zhou Y et al (2014) MicroRNA directly enhances mitochondrial translation during muscle differentiation. Cell 158:607–619. https://doi.org/10.1016/j.cell.2014.05.047